

Experimental Observation on Air-Conditioning Using Radiant Chilled Ceiling in Hot Humid Climate

Ashmin Aryal, Pipat Chaiwiwatworakul, Surapong Chirarattananon

Abstract—Radiant chilled ceiling (RCC) has been perceived to save more energy and provide better thermal comfort than the traditional air conditioning system. However, its application has been rather limited by some reasons e.g., the scarce information about the thermal characteristic in the radiant room and the local climate influence on the system performance, etc. To bridge such gap, an office-like experiment room with a RCC was constructed in the hot and humid climate of Thailand. This paper presents exemplarily results from the RCC experiments to give an insight into the thermal environment in a radiant room and the cooling load associated to maintain the room's comfort condition. It gave a demonstration of the RCC system operation for its application to achieve thermal comfort in offices in a hot humid climate, as well.

Keywords—Radiant chilled ceiling, thermal comfort, cooling load, outdoor air unit.

I. INTRODUCTION

HOT humid climate and low air movement make air-conditioning by cooling essential for the provision of human comfort in buildings in Thailand [1]. The traditional mixed-air system is used to cool and circulate the entire air in air-conditioned rooms which is energy-intensive. It was reported that about 60% of the electricity used in commercial offices in Thailand was shared by the air-conditioning system [2].

Radiant cooling system is an alternative to energy intensive conventional all-air system [3]. Among various configurations, RCC is a system of the simplest installation for both new design buildings and existing buildings to be renovated. The RCC utilizes its cooled surfaces to absorb heat radiated from occupants, equipment, light lamps, objects, and other surfaces with higher temperatures. The room air in contact with the ceiling surfaces is also cooled by convection. The radiative heat transfer presents the dominant mechanism in the radiant room that possesses more than 50% of the total heat absorbed by the RCC [4]. As the RCC can deal only with the sensible load, it must operate in conjunction with an outdoor air unit (OAU) to handle all latent load, hence establishing RCC as a hybrid system. By the distinct concept of these two systems, this paper carried out a physical experiment of the RCC system to investigate its operation and the resultant indoor thermal environment under a hot humid climate of Thailand. Past research showed an inability of the radiant system to use chilled

water below 24 °C under natural ventilation due to condensation [5]. The inability of a radiant system to handle the latent load and its dependence on thermal load, building structure, hydronic system [6], and impacts on thermal comfort make it a complicated venture. These have been recognized by experienced professionals and are the stumbling block in the penetration of the radiant system application in Thailand. The performance of the radiant system and its suitability depend on different climatic conditions [6], [7]. These induced a motivation to study the application of the RCC integrated with an outdoor air system for office buildings in tropical Thailand. The saturation of building in the forthcoming future and the shifting of the building to net-zero and ultra-low energy houses in the future adds to the importance of this study as well.

II. EXPERIMENTAL SETUP

A. Experimental Room

An outdoor chamber, situated on the roof deck of the building of the School of Bio-resources and Technology, King Mongkut's University of Technology Thonburi, was used as the experimental site. The chamber was a rectangular shape of width 3.0 m, length 9.0 m, and a height of 2.6 m measured from the floor to ceiling. The width sides of the room faced to the north and the south. Both walls (the north and the south) were equipped with double-pane windows of 4 mm thick green glasses. The window was 1.5 m high. External shading slats were installed to intercept the intense beam radiation to reduce the window heat gain. All opaque wall parts were insulated with polystyrene foam (PS) of 0.1 m thickness, covered with 0.01 m gypsum board on both sides. The roof is a 3 mm thick aluminum sheet under which 0.15 m PS and 0.012 m gypsum were affixed. The floor was made from cement fiber and particle board of 0.02 m thickness. The room interior was refurbished to create an office-like environment.

B. Radiant Cooling System

The installed radiant system was a hybrid of chilled ceiling panels and an OAU. The system diagram is presented in Fig. 1. An inverter-type air-cooled chiller of 12.2 kW_{th} cooling capacity was used to produce chilled water at 7 °C and supply it to an OAU that was responsible to handle the latent loads from the outside air and inside the experimental room. The OAU circulated the air at a constant flow of 100 CFM through

P. Chaiwiwatworakul is Assoc. Prof at Energy Division, Joint Graduate School of Energy and Environment (JGSEE), King Mongkut's University of Technology Thonburi (KMUTT); and Center for Energy Technology and Environment (CEE), (corresponding author, e-mail: pipat_ch@jgsee.kmutt.ac.th).

its cooling coil where 50 CFM were the outdoor air intake, and another 50 CFM was the room air. An automatic 2-way valve was used to regulate the chilled water flow to the cooling coil by using the signal from PT100 sensor to maintain the room air

temperature (T_a) to meet the setpoint value. To enhance the dehumidification, the OAU coil was equipped with a wrap-around heat pipe heat exchanger that pre-cooled the entering air and re-heat the leaving air of the coil.

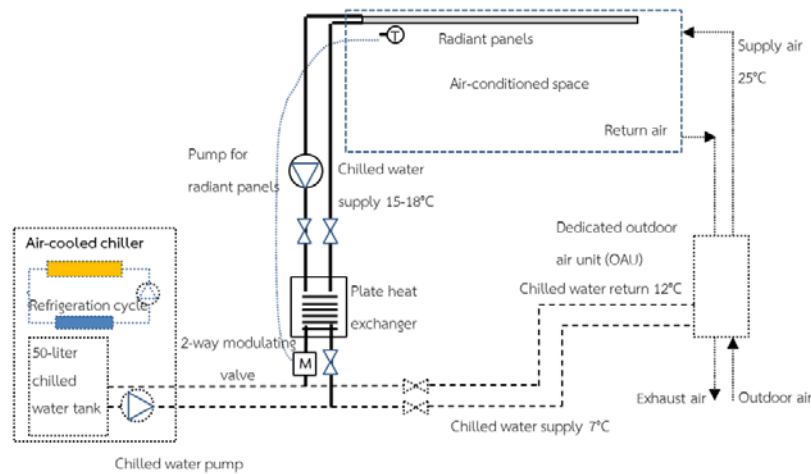


Fig. 1 Chilled water circuit of the radiant system

The chilled water from the chiller was also supplied to a plate heat exchanger. The heat exchanger was equipped with a motorized valve to control the surface temperature of the ceiling panels (T_{rep}) according to the setting value. A pump was used to circulate the chilled water at a constant rate of 0.175 kg/hr in the radiant panel loop.

In the laboratory, the ceiling panels are composed of several aluminum blade profiles acting as fins onto which copper tube was affixed. A manifold was used to distribute the supply water equally to the five panels, each connected in parallel in the water circuit. The chilled ceiling panel absorbs heat from the room by radiation and convection.

A 50-liter water tank was installed to store the chilled water for stabilizing the chilled water temperature during the system operation.

C. Measurements

TABLE I

DIFFERENT SENSORS AND MEASUREMENT IN THE RADIANT ROOM

Items	Parameters	Sensor	Measurement
1	Interior and exterior temperature	Thermocouple K type	Continuous
2	Panel surface temperature	PT-100	Continuous
3	Air temperature and relative humidity	Temperature and humidity sensor	Continuous
4	Airspeed	Anemometer	Spot
5	Water temperature	PT-100	Continuous
6	Water flow rate	Water flow meter	Spot
7	Heat flux	Heat flux sensor	Continuous

Several sensors were installed to measure the indoor condition including the room temperature, relative humidity, globe temperature, and wall surface temperature. The radiant system operating parameters were also measured i.e., the chilled water flow rate, supply and return chilled water temperature, and heat flow of the chilled ceiling panel. The

measured data were recorded every one minute by a data logger. Table I gives a list of the measurement and the installed sensors.

D. Load Calculation of the Chilled Ceiling

The measured data from the sensors were employed to determine the heat absorption of the RCC panels. The amount of the absorbed heat by the radiative exchange (q_{ri}) was calculated based on the radiosity/irradiation method (RIM) [8].

The net radiant energy received by the surface e.g., the RCC panel and other surfaces in the radiant room is given by:

$$q_{ri} = \frac{\varepsilon_i}{1 - \varepsilon_i} (E_{bi} - J_i), \quad (1)$$

where, ε_i , E_{bi} , J_i are emittance, black body emissive power, and radiosity for surface i in the radiant room.

The total radiation flux J_i from a surface i is called radiosity. As expressed by (2), the radiosity can be defined as the sum of the emitted radiation of the surface i and the reflected radiosity from all other surfaces in the enclosure:

$$J_i = \sigma \varepsilon_i T_{ai}^4 + \rho S_i, \quad (2)$$

where $S_i = \sum_{j=1}^n F_{ij} J_j$, is the sum of radiation from all other surfaces reaching surface i . ε is the surface emittance. σ is the Stefan Boltzmann constant of 5.67×10^{-8} . F_{ij} is the form factor from the surface i to surface j . T_{si} is the temperature of the surface i . In the calculation, the emittances of all surfaces were assumed equal to 0.8 while that of the panel was kept as 0.9. So

$$J_i = \sigma \varepsilon_i T_{ai}^4 + \rho \sum_{j=1}^n F_{ij} J_j. \quad (3)$$

Equation (3) can be written in matrix form as:

$$\begin{bmatrix} 1 - \rho_1 F_{11} & -\rho_1 F_{12} & - & - & - \\ -\rho_1 F_{11} & 1 - \rho_2 F_{22} & -\rho_2 F_{23} & - & - \\ - & - & - & - & - \\ - & - & - & - & - \\ -\rho_n F_{n1} & - & - & - & 1 - \rho_n F_{nn} \end{bmatrix} \begin{bmatrix} J_1 \\ J_2 \\ - \\ - \\ J_n \end{bmatrix} = \begin{bmatrix} \epsilon_1 \sigma T_{a1}^4 \\ - \\ - \\ - \\ \epsilon_n \sigma T_{an}^4 \end{bmatrix}$$

Solving the above matrix, J_i and S_i can be calculated. Thus, the net radiant energy received by the RCC panel ($q_{rp,rad}$) and other surfaces in the radiant room can be obtained by using (1).

The estimation of the absorbed heat by convection ($q_{rp,conv}$) was calculated using the following equation for a cooled surface facing downward [2]:

$$q_{rp,conv} = 1.52(T_a - T_{p,avg})^{\frac{1}{3}} \quad (4)$$

where, T_a is the room air temperature, and $T_{p,avg}$ is the RCC panel surface temperature.

The sum of $q_{rp,rad}$, and $q_{rp,conv}$ was considered as the total heat absorbed by the radiant ceiling panel. The rate of water flow in the panel (m_c) and the temperature difference between chilled water return temperature from the panel ($T_{rp,chw}$) and chilled water supply ($T_{rp,chws}$) to the panel could be used to calculate the heat gained by the panel from the room:

$$Q_{rp} = m_c S(T_{rp,chw} - T_{rp,chws}) \quad (5)$$

where S is the specific heat capacity of water.

By using (5), it could be calculated the heat gained by the OAU (Q_{oau}). The cooling load of the room was the sum of Q_{rp} and Q_{oau} . Q_{oau} could further be divided into the sensible load ($Q_{oau,s}$) and latent load ($Q_{oau,l}$)

E. Thermal Comfort Assessment

The thermal comfort inside the room was assessed by using Fanger's PMV index [9] prescribed in ASHRAE 55 [10]. The PMV was based on four physical variables and two personal variables. The physical variables dry-bulb temperature, relative humidity, air velocity and mean radiant temperature were measured by the sensors inside the radiant room whereas the metabolic rate of 1.2 met and the clothing insulation of 0.5 clo were employed for the calculation.

In the experiment, to imitate three occupants staying in the experimental room, a wooden casing containing fluorescent lamps inside was placed at the room center. The lamps were turned on during the operating office hours to generate the longwave sensible heat of 252 W_{th} through the casing surface. A humidifier was used to produce a mist of 0.32 kg/hr to imitate the latent heat.

III. RESULT AND DISCUSSION

Experiments were undertaken for several days to investigate the thermal environment in the radiant room. However, only the experiment on 22 October 2020 was chosen to present in this paper. Fig. 2 shows the ambient condition of the experimental day. The solar radiation was very intense; the global radiation exceeded 1,000 W/m² during noon. Over the day, the outdoor air temperature varied between 24 °C and 30 °C. The dew point temperature reached its maximum at 23.4 °C. These

measurements portray a hot and humid day in a tropical region.

A. Experimental Results

The OAU was run from 8:40 till 16:05 to dehumidify the room air. Fig. 3 (a) shows the conditions of the OAU supply and return air. During the operation, the supply air temperature ($T_{s, oau}$) was about 20 °C. The humidity ratio ($W_{s, oau}$) varied between 9-11 g_w/kg_{da}, corresponding to the dew point temperature of 15 °C. The OAU spent 55 minutes to reduce the room humidity ratio ($W_{r, oau}$) from 17 g_w/kg_{da} to 11 g_w/kg_{da}. It should be remarked that during the system startup period, the outdoor air damper was shut-off and the OAU dehumidified the room air only. The room air was also cooled down from a temperature of 28 °C to 24 °C. The temperature and humidity of the outdoor air were given in the plot for a comparison with the indoor air.

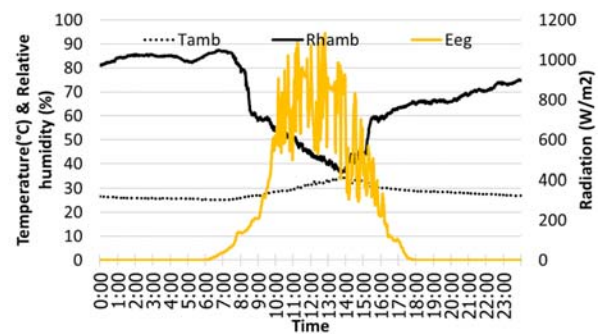
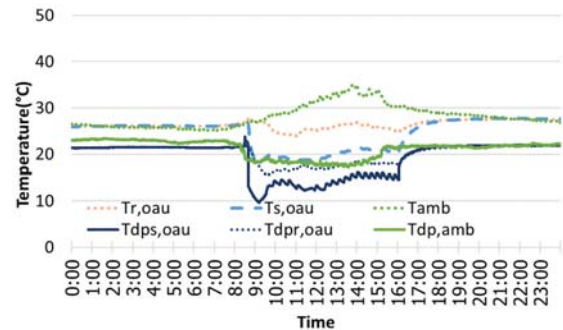
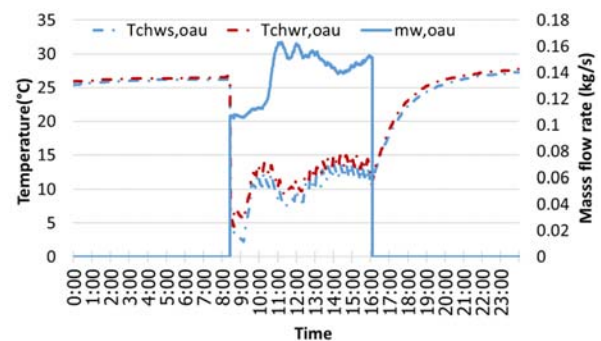


Fig. 2 The outdoor condition (22 October 2020)



(a) Supply and return air



(b) Chilled water

Fig. 3 The OAU condition measurements

Fig. 3 (b) presents the chilled water flow of the OAU. The flow rate was adjusted by the motorized valve to meet the control set point. The temperature of the OAU supply chilled water ($T_{chws, oau}$) varied during the operation period (8:40-16:05); from 5 °C in the morning up to 14 °C in the afternoon. This is the result of the inverter chiller having a large cooling capacity, which did not have a proper match with the low thermal load of the experimental room.

In Fig. 3 (b), after the chilled water taking the load from the OAU coil, its temperature increased 2-3 °C from the supply temperature. The calculation done by using the chilled water data reported that the load at the OAU was about 1 kW_{th}. It can be noticed that the chilled water in the system pipe raised to 26-28 °C during the system shut-down.

Next, the experiment room condition was examined as shown in Fig. 4. The setpoint of the radiant ceiling surface temperature was fixed at 19 °C during the experiment. As mentioned earlier, five ceiling panels were installed in the experimental room; however, only the average temperature ($T_{p,avg}$) was given in the plot. With our PID control, the panel temperature had a large fluctuation (17-22 °C) before it approached the set point. The supply temperature of the chilled water was 12-18 °C whereas the return temperature was 3 °C higher than the supply temperature. The chilled water pipe used in the experimental room was polypropylene random copolymer (PPR) with inherent insulation property. This helped to prevent condensation on the pipe surface. There was no condensation on the ceiling, as its surface temperature was higher than the room dew point temperature throughout the experiment.

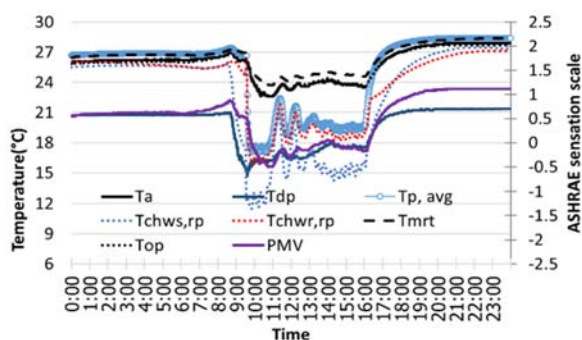


Fig. 4 The room condition measurements

By the RCC system operation, the room air (T_a) could be maintained within a small variation of 23-24 °C. The slightly increasing temperature in the afternoon resulted from the higher external load, whereas the OAU supply air temperature and the ceiling surface temperature were kept constant.

The mean radiant temperature (T_{mrt}) is defined as the uniform temperature of an imaginary enclosure in which the radiant heat transfer from the human body is equal to the radiant heat transfer in the actual non-uniform enclosure [11]. It can be estimated in different ways. In this study, the mean radiant temperature was calculated by using the measured surface temperature of all interior walls with respect to the room center. The experiment reported that the mean radiant temperature

(T_{mrt}) of the room was higher than that of the room air. This result might be distinct from other experimental studies [12]-[14]; however, it could be explained that all walls of the experimental room were exposed to the outdoor environment.

By using the measured data of the physical room condition and assuming the personal variables of the sedentary activities 1.2 met and the clothing insulation level 0.5 clo, the thermal comfort level based on ASHRAE sensation scale could be calculated and presented in Fig. 4. The predicted mean vote (PMV) varied between -0.5 to 0 indicating a large group of people felt marginally cool. The calculated predicted percentage of dissatisfied (PPD) was within 10%.

The experiment also investigated the cooling load characteristic of the RCC system. At first, the heat absorbed by the front surface of the ceiling panels (the surface facing downward) was examined. Fig. 5 portrays the absorbed heat measured by a heat flux sensor attached to the panel front surface ($Q_{rp,fr,hf}$). The heat amount varied between 30-70 W/m². Fundamentally, the ceiling panel absorbed heat by radiative exchange with objects and wall surfaces in the room interior and by convective exchange with room air (as in Fig. 6). With this regard, one could estimate the heat absorption on the panel front surface by using (1)-(4). The calculated results of the absorbed heat by radiation ($q_{rp,rad}$) and by convection ($q_{rp,conv}$) were given in Fig. 5. The total absorbed heat shown in the plot from the calculation ($q_{rp,t}$) is in good agreement with the measured result from the heat flux sensor. It can be observed that the radiative heat gain from the panel was around 80% of the total heat gained by the panel. This value was close to the result obtained by other researchers [12], [13].

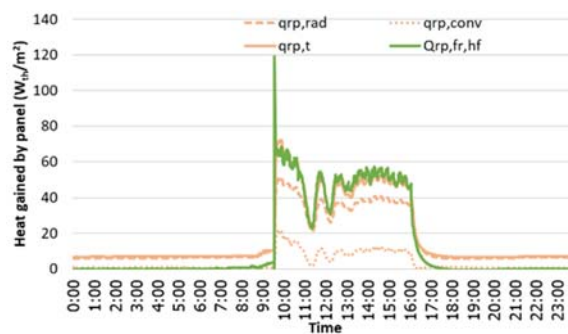


Fig. 5 Heat absorption by the front surface of the ceiling panel

For further analysis, the total heat absorbed by both sides of the ceiling panel was considered. The total heat absorbed by the panel was obtained by two different means: (M1) the direct measurement using heat flow sensors (HF1 and HF2) attached on the front and backside of panel surfaces (as shown in Fig. 6) and (M2) the calculation using the measured data from chilled water side i.e., the flow rate of chilled water and its corresponding supply and return temperature.

Fig. 7 illustrates the heat absorbed by the ceiling panel obtained by the two means of M1 and M2. $Q_{rp,fr,hf}$, and $Q_{rp,bk,hf}$ are the measurements of heat flux sensors on the front surface and on the backside of the ceiling panel, respectively. The proportion of the heat on the front side and the backside was 80:

20. The sum of the two heat flux measurements ($Q_{rp,t,hf}$) did well agree with that of the heat calculated from the waterside ($Q_{rp,ws}$). Fig. 7 also shows that the amount of the absorbed heat was relatively high when the RCC system started and the room had high thermal load conditions. The absorbed heat was dependent on its surface temperature. On an experimental day, the absorbed heat of the chilled ceiling was averaged at 70 W/m^2 .

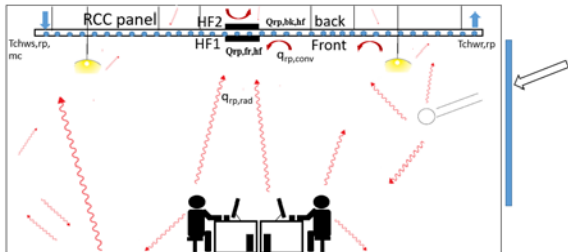


Fig. 6 Calculation of heat absorbed by a panel using the heat flux sensor and from the waterside

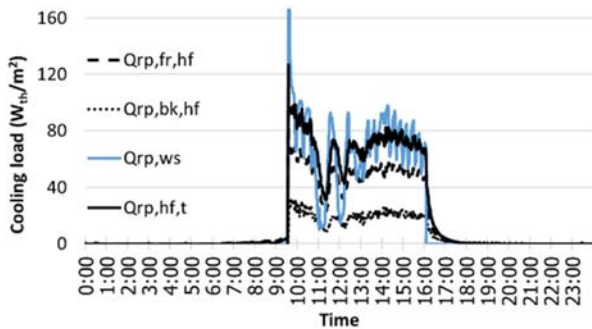


Fig. 7 Measurements of the ceiling heat absorption

Fig. 8 depicts the total cooling load of the RCC system taken by the ceiling panels and by the OAU. The cooling load at the panel was 2.5 kW_{th} while that of the OAU was 1 kW_{th} . As the floor area of the experimental room was 27 m^2 , the room cooling load was $130 \text{ W}_{th}/\text{m}^2$.

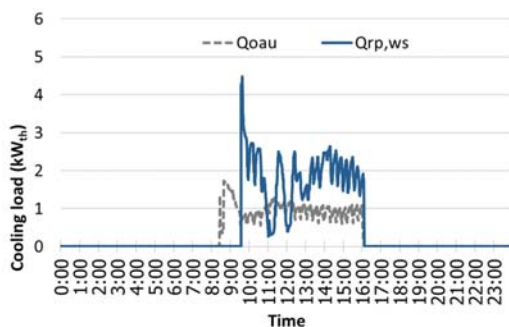


Fig. 8 Total cooling load of the RCC system

IV. CONCLUSION

Air-conditioning using a radiant system was studied experimentally in a full-scale outdoor laboratory chamber. In its application in a hot humid climate, integrated energy-efficient measures i.e., wall insulation, sun shading, daylighting, energy

recovery were implemented to reduce the cooling load and to improve the indoor thermal environment. To successfully operate the chilled ceiling without condensation, the moisture level of the radiant room was controlled with the help of ventilation and recirculation air dehumidified by a cooling coil of a dedicated OAU. A wrap-around heat pipe heat exchanger was integrated into the cooling coil to enhance the dehumidification performance and the cooling capacity of the radiant panel. The OAU could reduce the room dew point temperature for starting the chilled ceiling within 1 hour. The chilled ceiling panels shared the load as high as 70% of the total cooling load. The RCC system operation provided the neutrality of thermal comfort of the radiant room at the operative temperature of $24 \text{ }^\circ\text{C}$.

ACKNOWLEDGMENT

The financial support from the National Science and Technology Development Agency (NSTDA), grant no. P-16-51993 through this research project is gratefully acknowledged.

REFERENCES

- [1] S. Chirattananon and V. D. Hien, "Thermal performance and cost effectiveness of massive walls under thai climate," *Energy Build.*, vol. 43, no. 7, pp. 1655–1662, 2011.
- [2] Surapong, Chirattananon, "Building for Energy Efficiency." (Energy Field of Study, School of Environment Resources and Development) 2005, pp. 616.
- [3] A. Aryal, P. Chaiwiwatworakul, and S. Chirattananon, "A simulation study of radiant chilled ceiling with dedicated outdoor air system for office buildings in Thailand," *IOP Conf. Ser. Mater. Sci. Eng.*, vol. 965, p. 012004, 2020.
- [4] K. N. Rhee, B. W. Olesen, and K. W. Kim, "Ten questions about radiant heating and cooling systems," *Build. Environ.*, vol. 112, pp. 367–381, 2017.
- [5] P. Vangtook and S. Chirattananon, "An experimental investigation of application of radiant cooling in hot humid climate," *Energy Build.*, vol. 38, no. 4, pp. 273–285, 2006.
- [6] Y. Khan, V. R. Khare, J. Mathur, and M. Bhandari, "Performance evaluation of radiant cooling system integrated with air system under different operational strategies," *Energy Build.*, vol. 97, pp. 118–128, 2015.
- [7] Y. Khan, M. Bhandari, and J. Mathur, "Energy-saving potential of a radiant cooling system in different climate zones of India," *Sci. Technol. Built Environ.*, vol. 24, no. 4, pp. 356–370, 2018.
- [8] M. M. Ardehali, N. G. Panah, and T. F. Smith, "Proof of concept modeling of energy transfer mechanisms for radiant conditioning panels," *Energy Convers. Manag.*, vol. 45, no. 13–14, pp. 2005–2017, 2004.
- [9] P.O. Fanger, "Assessment of Thermal Comfort," *Br. J. Ind. Med.*, vol. 30, pp. 313–324, 1978.
- [10] ANSI/ASHRAE, "Thermal Environmental Conditions for Human Occupancy," vol. 2017, 2017.
- [11] N. Nutprasert and P. Chaiwiwatworakul, "Radiant cooling with dehumidified air ventilation for thermal comfort in buildings in tropical climate," *Energy Procedia*, vol. 52, pp. 250–259, 2014.
- [12] J. Miriel, L. Serres, and A. Trombe, "Radiant ceiling panel heating-cooling systems: Experimental and simulated study of the performances, thermal comfort and energy consumptions," *Appl. Therm. Eng.*, vol. 22, no. 16, pp. 1861–1873, 2002.
- [13] S. Okamoto, H. Kitora, H. Yamaguchi, and T. Oka, "A simplified calculation method for estimating heat flux from ceiling radiant panels," *Energy Build.*, vol. 42, no. 1, pp. 29–33, 2010.